JOURNAL OF MATERIALS SCIENCE 24 (1989) 4080–4087

Corrosion of hot pressed silicon nitride-based materials by molten copper

R. SANGIORGI*, A. BELLOSI‡ , M. L. MUOLO*, G. N. BABINI‡
*CNR-ICFAM, Istituto di Chimica Fisica Applicata dei Materiali, Lungo Bisagno Istria 34, Genova, Italy
‡CNR-IRTEC, Istituto di Ricerche Tecnologiche per la Ceramica, Via Granarolo, 64 – Faenza, Italy

The behaviour of several types of silicon nitride–based materials in contact with molten copper has been evaluated. Tests were performed at a temperature of 1400 K for a holding time of 260 h in fluido-dynamic conditions.

The extent of corrosion has been evaluated in terms of linear loss, weight loss, morphology and chemical composition of the surfaces remaining in contact with the molten phase, by means of SEM, EPMA and X-ray diffraction. Corrosion resistance has been found to be a function of the chemical composition, type and amount of the secondary phases. Materials produced with MgO as a sintering aid showed poor resistance whereas those with Al_2O_3 exhibited the best performance. In any case the extent of corrosion was very slight and the results revealed that all the tested ceramics may be considered suitable for use in contact with molten copper.

1. Introduction

Silicon nitride is a ceramic of considerable interest because it possesses a number of chemical, physical and mechanical properties which endow it with numerous potential uses.

In some of the high temperature engineering applications which have been considered for silicon nitride, the ceramic material could be in contact with molten metals. For example, in the metallurgical industry silicon nitride-based materials have been proposed for use as containers, nozzles, drawing dies and other structural components.

The possibility of a metal–ceramic reaction at high temperatures must be considered, as well as the affect of this reaction on the material's properties. A detailed knowledge of the nature and severity of the reactions, of the factors influencing the attack and the characteristics of the reaction products is needed.

Concerning the complex interaction which occurs in metal matrix composites, silicon nitride whiskers have been shown to react with aluminium, iron and nickel at high temperatures [1–3]. Studies have been reported on the reactions among silicon nitride and several metals [4, 5]. The observations were directed to the phenomenology and the evaluation of such questions as the temperature for onset of reaction, the severity of the attack and the nature of the reaction products.

As far as the behaviour of silicon nitride with molten copper is concerned few studies exist. Silicon nitride has been reported to be non-compatible [6, 7], whereas sialon crucibles were unaffected by molten copper [8, 9].

The purpose of the current study is to survey the chemical interaction between molten copper and various silicon nitride-based ceramics. Such ceramics are multiphase materials and the mechanisms of corrosion are complex, depending on microstructural parameters, in particular on the type and amount of secondary phases.

In the frame of investigations on the wettability of silicon nitride by copper, the materials involved had shown satisfactory values of contact angle and of work of adhesion [10].

For the corrosion tests, various silicon nitride ceramics were chosen, which varied considerably in terms of type and amount of secondary phases, microstructure and specific thermal and mechanical properties [11–14], so as to acquire a clear understanding of the physicochemical processes involved in the interaction with molten copper.

2. Materials

The composition and microstructural parameters of the tested materials are shown in Table I. A detailed description of hot pressing conditions and of various physicochemical properties are given elsewhere [11–15].

A brief description of the most important features affecting interaction with metal is given below.

(i) Material M is nearly fully dense, the intergranular phase (~ 6 vol %) [11] is mainly composed of glassy and crystalline magnesium silicates, were (calcium, iron, aluminium) impurities of the starting Si_3N_4 powder segregate.

(ii) The intergranular phase of sample YM (~ 12 vol %) has partially crystallized to yttrium silicates, to yttrium oxynitrides and to yttrialite, a solid

0022–2461/89 $03.00 + .12

TABLE I Characteristics of the tested materials

	Additives wt %	Hot pressing conditions			Density ($g\,cm^{-3}$)	Relative density (%)	Mean grain size (μm)	Residual α-Si_3N_4 phase (%)		Secondary phase (ZrO_2)	Intergranular phases
		T (°C)	P (MPa)	t (min)							
M	3 MgO	1650 +	34.4	10	3.19	99.6	0.55	7.80			mainly glassy
MY	1MgO–8Y_2O_3	1750	34.4	60	3.21	97.9	0.92	2.0			$YNSiO_2$; Yttrium silicates
A	5Al_2O_3	1650	34.4	120	3.13	98.0	0.85	40.0	0.60		Si_2N_2O; SiAlON
AZ	5Al_2O_3–12ZrO_2	1650	34.4	120	3.31	97.0	0.85	26.0	0.74	13m-ZrO_2; 8t-ZrO_2	Si_2N_2O; X-SiAlON

Si_3N_4: Starck LC12; MgO: Merck; Y_2O_3: Reidel de Haen; Al_2O_3: Alcoa A 16; ZrO_2: Harshaw.

solution of yttrium silicate and several cations (calcium, aluminium, iron).

(iii) The intergranular phase amount of materials A and Az is very scarce, as the densification aid (Al_2O_3) enters s.s. with Si_3N_4 to form β'-sialon. The presence of β'-sialon proved to be strictly correlated to a lot of thermochemical properties [12].

(iv) Material AZ is a composite Si_3N_4–ZrO_2 where ZrO_2 is distributed in the Si_3N_4 matrix in discrete particles (0.2 to 2 μm) and does not take part in the formation of the intergranular phase, at least in detectable amounts. β'-sialon is also present.

3. Methods

The silicon nitride samples were diamond cut from the hot pressed billetts, wet polished with various grades of diamond paste up to 1 μm, and ultrasonically cleaned.

Corrosion tests consisted of bathing silicon nitride-based materials billets in liquid copper. Two sets of four different billets were mounted on a graphite holder, a photograph of which is shown in Fig. 1. The holder was put in a graphite crucible and 99.98% copper shots were added: the crucible was then inserted in a vacuum furnace. A detailed description of the testing device is given by Sangiorgi *et al.* [16]. The size of the billets was about 4 × 4 × 20 mm^3 and the copper bath weighed about 300 g. When the copper had been melted under a 10^{-3} Pa vacuum, the furnace was filled with helium at a pressure of 6 × 10^4 Pa, in order to minimize the evaporation loss of copper, then the sample holder was allowed to rotate at speed of 1 r.p.m. (taking into account the dimension of the holder, this speed corresponds to a linear velocity of

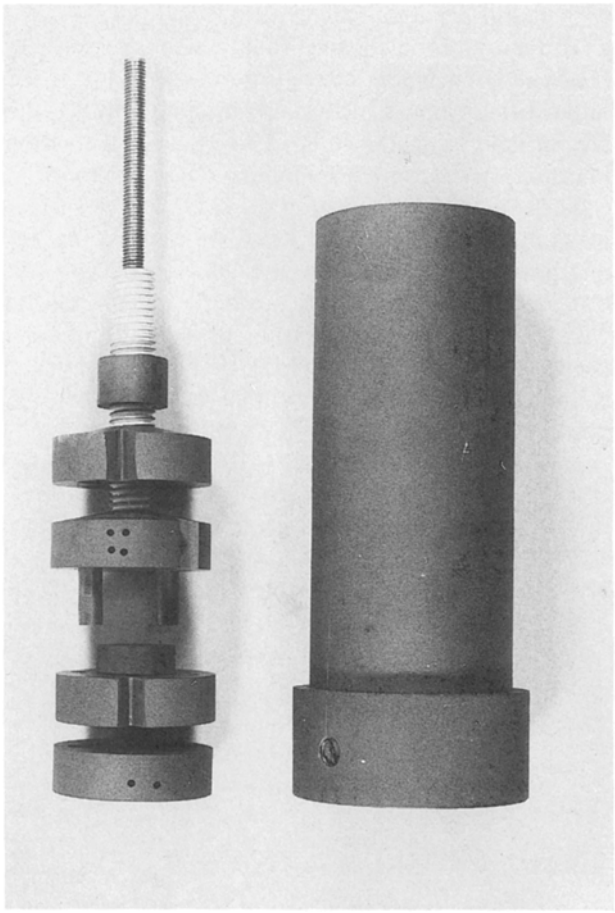

Figure 1 Graphite holder used for the corrosion tests.

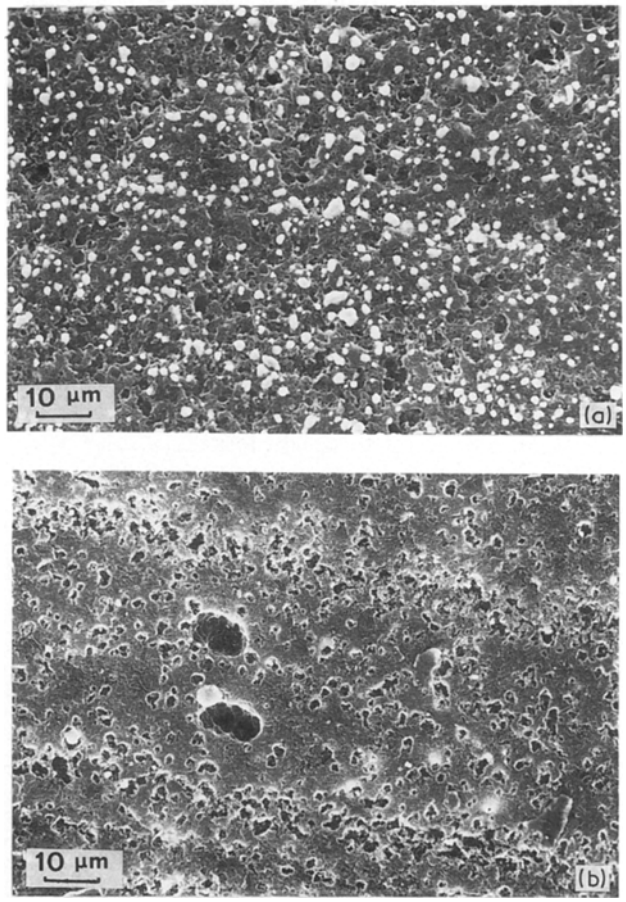

Figure 2 Surface morphology of material M after corrosion tests: (a) a lot of pits have been formed; (b) area where copper-based spherulitic particles adhere.

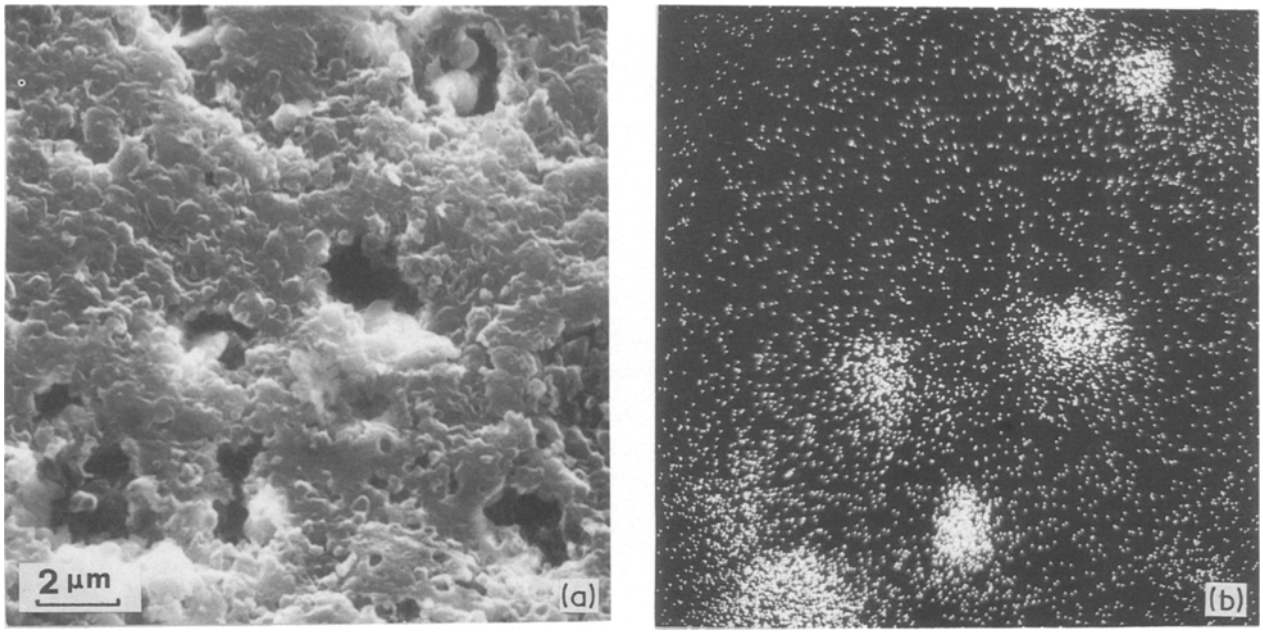

Figure 3 (a) The morphology of pits on sample M and (b) the X-ray map of copper.

about 1.25 mm sec^{-1}). The samples were held for 260 h at a temperature of 1400 K. When the holding time was over, the sample holder was raised so that its upper part remained out of the liquid copper, then the furnace was turned off. The set of specimens contained in the upper part of the holder were measured by means of a metrological microscope with an accuracy of $\pm 1\,\mu$m, and weighed (to an accuracy of ± 0.1 mg) and then subjected to SEM, EPMA, and X-ray analysis. The specimens contained in the lower part of the holder remained embedded in the solidified copper. They were cut and polished using standard metallographic techniques and then submitted to SEM and EPMA analysis in order to evaluate the interfacial morphology.

The weight loss of the specimens has been expressed as the difference in weight before and after the run, divided by the area exposed to liquid copper.

4. Results

The interaction between silicon nitride-based materials and molten copper results in a very low weight loss (Table II) for samples M and YM. Materials A and AZ were not subject to weight loss.

The overall dimension of the specimens remained constant at a sensitivity of $\pm 5\,\mu$m, i.e. 0.1%.

In the following, references are made to two classes of materials (M, YM and A, AZ), according to their chemical resistance.

4.1. Materials with a lower chemical resistance

The external surface of specimen M that has been in contact with molten copper appears completely covered with pits, of different morphology and dimensions (Fig. 2a). In some areas, a lot of copper-based spherulitic particles adhere to the surface (Fig. 2b), mainly inside or around the pits (Fig. 3a, b); the interaction silicon nitride-copper has involved the transference of copper to the silicon nitride surface.

TABLE II Weight loss after corrosion tests

Sample	ΔW (mg)	S (cm^2)	$\Delta W/S$ mg cm^{-2}
M	−3.4	1.17	2.9
MY	−0.7	1.14	0.6
A	0	1.17	0
AZ	0	1.13	0

The surface of sample MY is covered by a layer (Fig. 4), where copper-based particles adhere (Figs 5a and c). A strong enrichment of yttrium and calcium is detected on the surface (Figs 5d and e). The layer is spalled and some pits are evident.

The microprobe chemical analyses of the surfaces (Table III) evidences concentration of additive and impurities cations. Calcium, magnesium and yttrium are diffused from the bulk of Si_3N_4 to the reaction interface through grain boundary phase channels.

The calcium concentration (~11%) on the surface of sample M is excessive since its presence in the intergranular phase is very low (only ~0.3 wt % of CaO in the starting Si_3N_4 powder), in comparison with magnesium concentration (3 wt % MgO have been added as densification aid); the amount of which is limited on the surface.

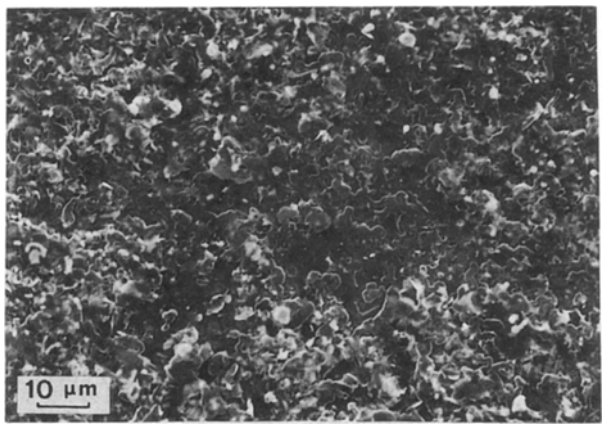

Figure 4 Surface morphology of material MY, where a surface thin layer has been formed.

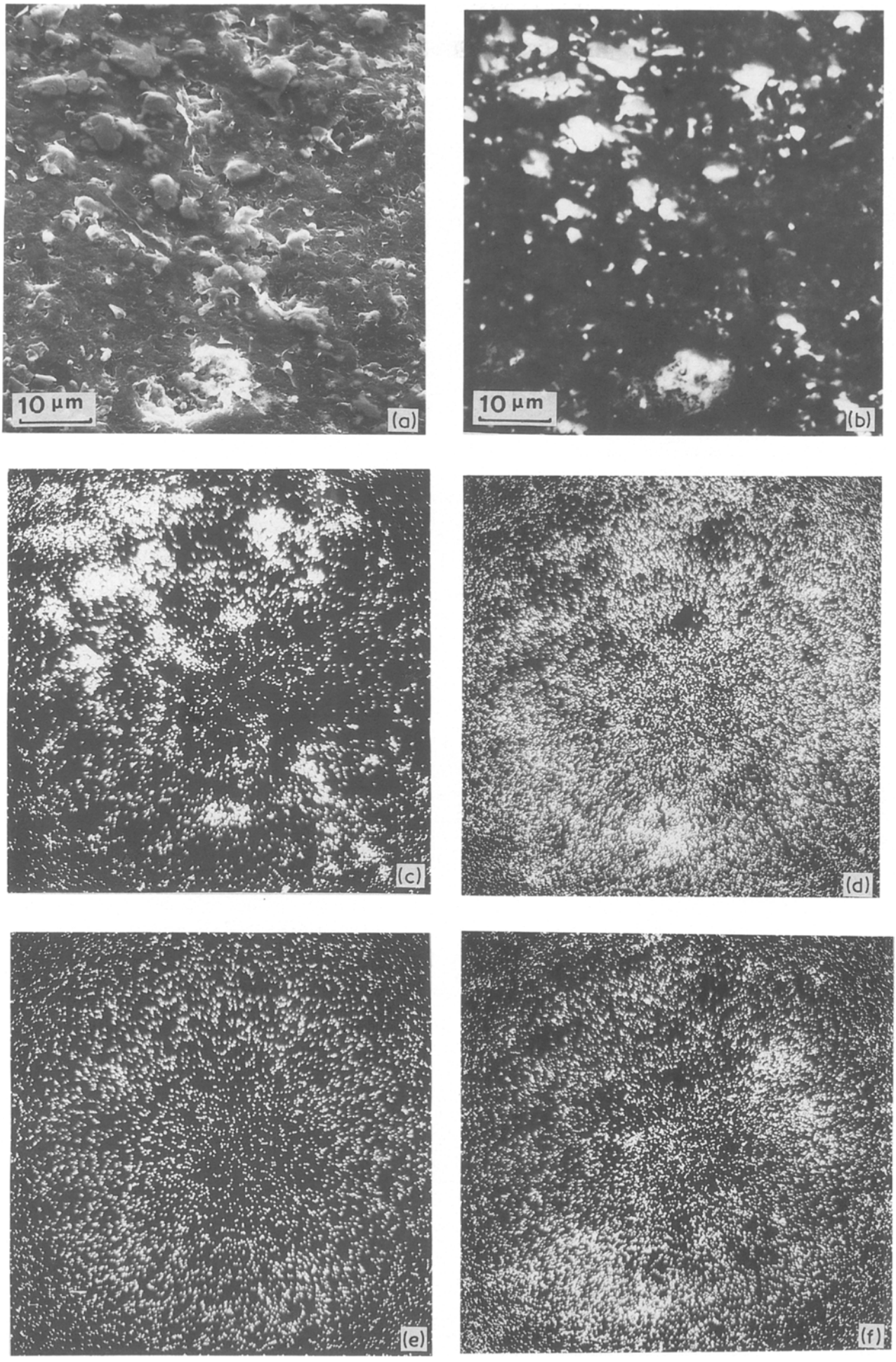

Figure 5 Surface of material MY after corrosion: (a) morphology, (b) back scattered electron image showing the distribution of the copper-based particles (white areas), (c) X-ray map of copper, (d) X-ray map of Y, (e) X-ray map of calcium, (f) X-ray map of silicon.

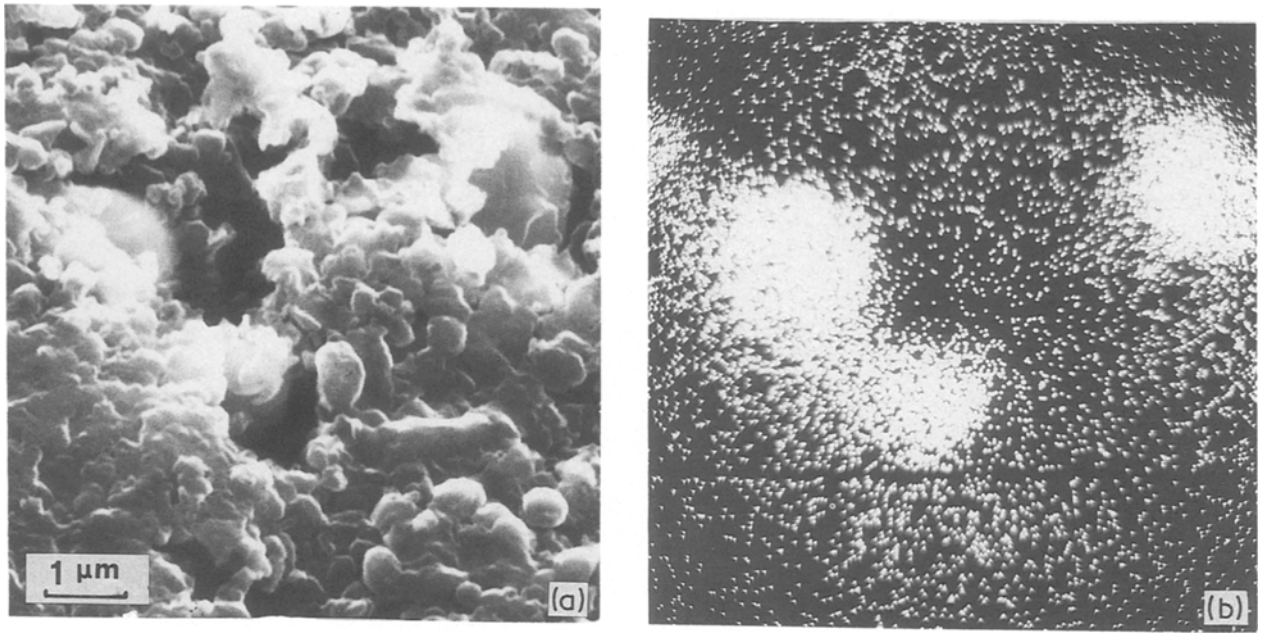

Figure 6 (a) Micrograph showing that copper enters the pits in material M; (b) X-ray map of copper.

Therefore it seems acceptable to suppose a reaction and dissolution of magnesium into liquid copper.

The interaction of copper with magnesium-reach intergranular phase is evident in Figs 6a and b, where copper, after having alloyed magnesium and produced pitting in the areas where the secondary phase concentrates, enter the pits and deepen the attack on silicon nitride through a further grain boundary phase decomposition. This phenomenology could give rise to some large ($\sim 50\,\mu m$) spalled areas observed on the surface of sample M (Fig. 7), probably in the areas of aggregation of secondary phase and/or porosity.

The behaviour observed occurs also in material MY, but the weight loss is lower than for M, probably owing to its lower content of magnesium an enhanced diffusion of yttrium from the bulk is detected (see Table III). The diffusion of calcium appears more scanty than for material M: this could be explained on the following basis

(i) The presence of yttrialite in the intergranular phase which holds calcium in solid solution.

(ii) A more crystalline and refractory character of the MY intergranular phase in comparison with that of the material M.

The chemical analysis of copper-based spherules on sample surfaces M and MY (Figs 8a and b) shows the presence of magnesium (up to 8 wt %), of silicon (up to 6 wt %) and of traces of calcium, aluminium, and also of yttrium in material MY.

The SEM and EPMA analyses of the cross-section of specimens M and MY did not show a heavy corrosion of the samples (Fig. 9a). The dark zone between ceramic and copper is a void which has been created during the cooling, because of the thermal mismatch between copper and silicon nitride. Traces of copper are detected on the surface of the ceramics as in Figs 9b and c, which are due to some copper-based particles adhering to the surface, as previously discussed.

Copper penetration in Si_3N_4 bulk via grain boundary phase channels has been detected up to $500\,\mu m$ from the reaction interface.

X-ray diffraction analyses show the presence, in addition to Si_3N_4 and copper, of a large number of minor reflections.

The evaluation of trace phases is very difficult on account of the partial overlapping of the peaks. However Cu_4Si in material M, and Cu_4Si, SiY, Cu_2Y in material MY can be identified.

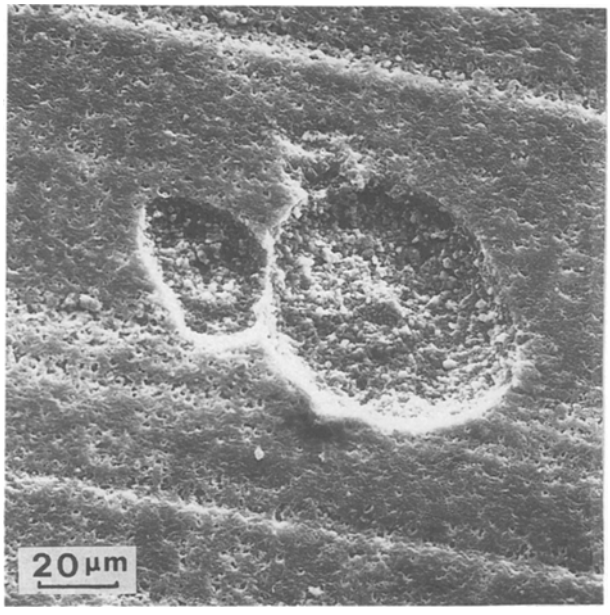

Figure 7 Large spalled areas on the surface of material M after corrosion.

TABLE III Chemical composition of the surface. Sample that remained in contact with molten copper. The reported values (wt %) represent a mean value of the results from various positions on the surface

Sample	Si	Mg	Y	Ca	Al	Zr	Cu
M	52	7		11			30
MY	43	1	40	2			14
A	30			30	10		30
AZ	15			7	4	70	4

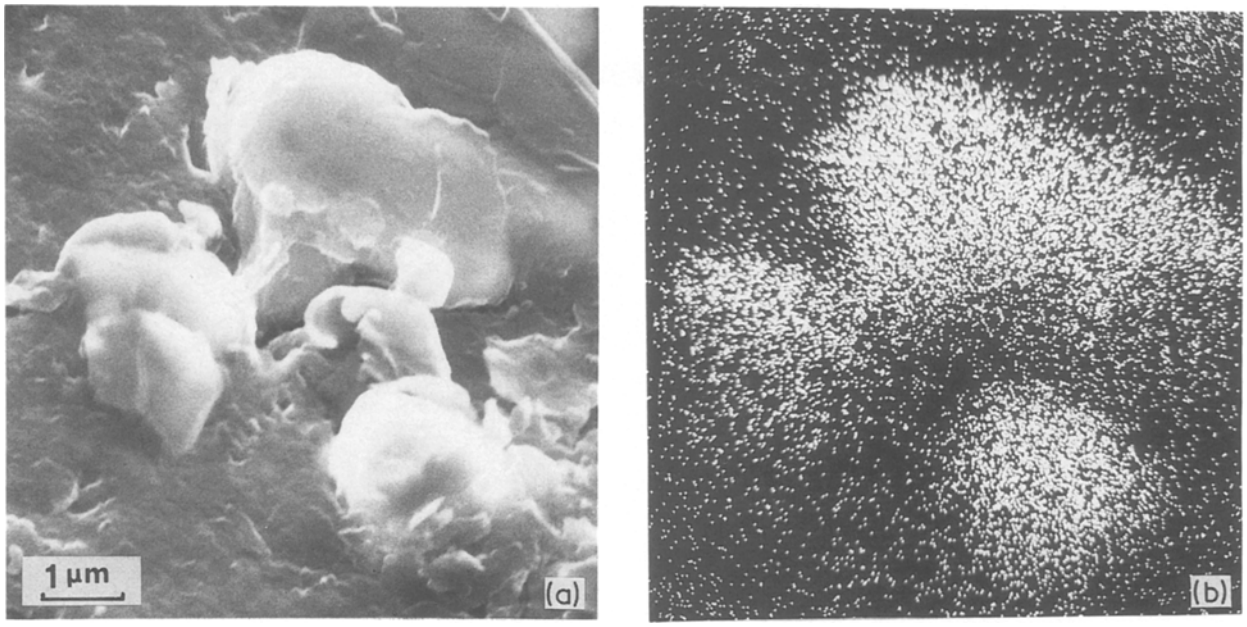

Figure 8 (a) Morphology of copper-based spherules on material M, (b) X-ray map of copper.

These compounds are not stable at the working temperature according to the phase diagrams [17] of the Cu–Me alloys. They form during the cooling of the liquid copper–silicon nitride, nevertheless their presence indicates that a silicon and yttrium uptake by copper occurred.

4.2. Materials with higher chemical resistance

The surface of A sample is almost entirely covered by a very thin layer (Fig. 10a), in which under high magnification microbubbles and micropores (up to $\sim 0.3\,\mu m$) are evident.

The layer on surface AZ is thicker and swellings, bubbles and cracks (up to $\sim 100\,\mu m$) have formed (Fig. 11b).

The very high concentration (Table III) of calcium (in A) and zirconium (in AZ) on the surface is consistent with microstructural features of these silicon nitrides: the sintering aid (Al_2O_3) is in solid solution with Si_3N_4 therefore a very poor intergranular phase remains, may be oxides and/or silicates, where only impurities (calcium, iron, aluminium) segregate. Among these only a massive diffusion of calcium occurs.

The analysis of the cross-section of samples A and AZ showed features very similar to those already discussed for specimens M and MY.

Copper penetrates in the Si_3N_4 bulk up to at least $\sim 20\,\mu m$.

In addition to silicon nitride and copper, the X-ray diffraction analysis of the surface indicates the presence of low quantities of Cu_5Si, CaSi, $CuAl_2$, $CaCu_5$, and, perhaps, $CaSiO_5$ in material A and of Cu_4Si, ZrSi, (Zr, Cu) phase and perhaps $Cu_4Zr_3Si_2$ and $Ca_2ZrSi_4O_{12}$, in material AZ.

Also in this case the remarks made before about the stability of Cu–Me compounds remain valid.

5. Discussion

Usually the corrosion of silicon nitride by molten metals and alloys [4, 5] is a complex phenomenon, which may be the result of several mechanisms whose simultaneous action depends on the characteristics of the material being processed and of the metal components.

The phenomena that cause corrosion are engendered and controlled by chemical reactions, decompositions and diffusion mechanisms [15].

Unfortunately reaction kinetics cannot be evaluated and it is impossible to indicate if the rate-controlling process is diffusion or reaction. Previous studies [5] suggest that the attack of silicon nitride by several alloys followed a linear rather than a parabolic rate law, indicating that the rate controlling process was primary reaction of Si_3N_4 with some alloy constituents (copper, iron, nickel). In the present case a further complication needs to be considered: the presence of grain boundary phase, that can greatly interfere with direct Si_3N_4–copper corrosion.

These factors emphasize the chemical characteristics (type and amount of intergranular phase) of Si_3N_4 and the presence of β'-sialon as the aspects that can be used to understand the comparative behaviour of the various materials. Such a role of the intergranular phase and of the β'-sialon were previously observed during the study of other properties like oxidation resistance [11, 13, 14] and chemical wear when employing Si_3N_4 cutting tools in cast iron machining [18].

The chemical and morphological analysis by SEM and EPMA of the corrosion product leads us to note that the Si_3N_4-based materials with intergranular phase containing magnesium show a weakness, albeit moderate, under attack by molten copper. On the contrary, material without this element in the intergranular phase and with the presence of β'-sialon shows a high resistance.

The same behaviour can be observed in the weight loss data, even if these should be taken with care. In fact they represent the difference in weight before and after the corrosion tests. As micrographs showed traces of copper spherulites on the surface of the samples, their weight could compensate losses.

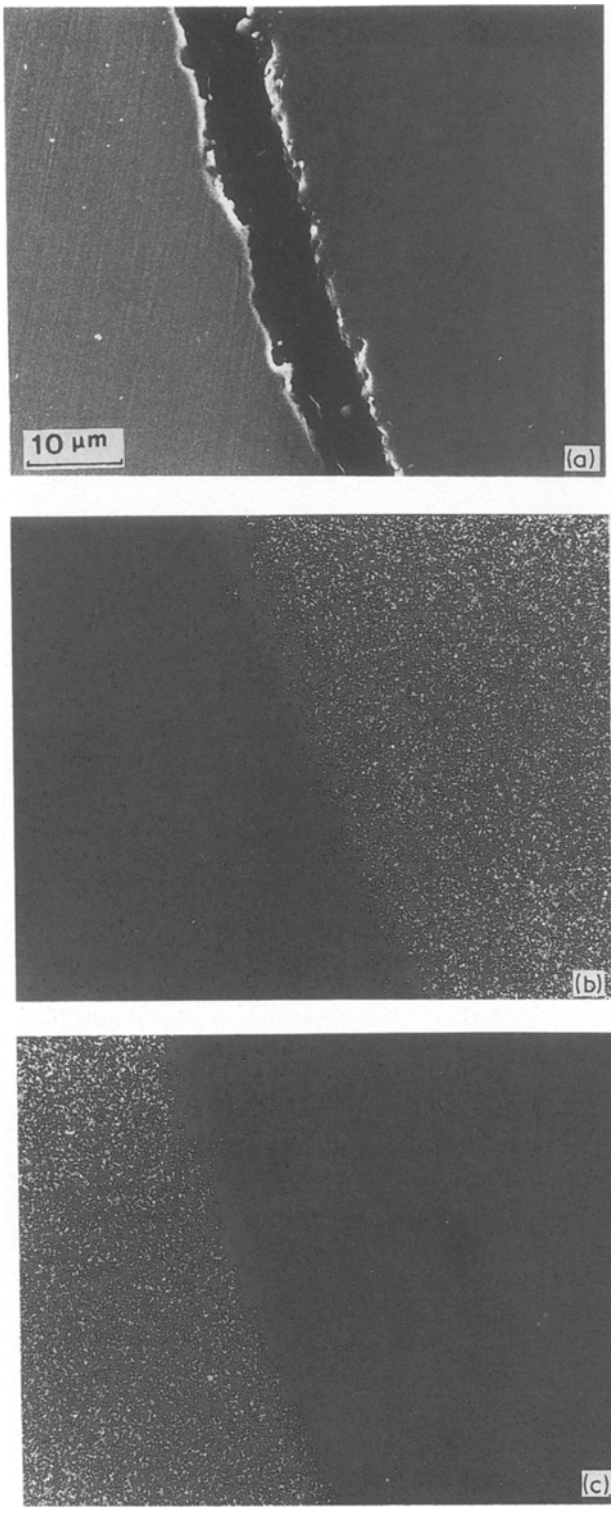

Figure 9 Cross-section of specimen M: (a) morphology, the dark zone between silicon nitride and copper is a void which has been created during the cooling because of the thermal expansion mismatch, (b) X-ray map of copper, (c) X-ray map of silicon.

The above examined results and the general chemical characteristics of the tested materials allow us tentatively to suggest a phenomenological model of interaction between molten copper and silicon nitride-based materials.

In the case of samples M and MY, magnesium is relatively free in the intergranular phase. It diffuses to the surface and could be taken up in the molten copper. The chemical attack on the secondary phase and the decomposition of magnesium-silicates constituting the grain boundary phase produce a pitting of the surface and allow the penetration of molten copper into the bulk, increasing the corrosion-reaction surface area.

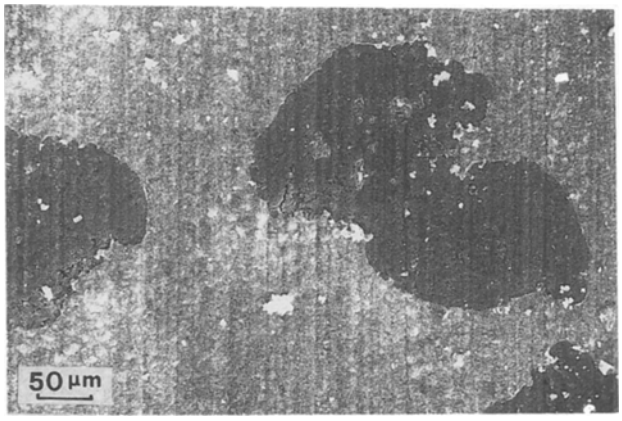

Figure 10 Morphological aspect of the surface of sample A after corrosion.

A diffusion similar to that of magnesium has been shown for all kinds of impurities, mainly calcium, owing to its high mobility in the intergranular phase, and for yttrium: these elements are transferred to the surface, where they remain.

In the case of A material the presence of Al_2O_3 in β'-sialon s.s. leads to a very poor intergranular phase, therefore a corrosion phenomenon could only arise from a direct attack of copper on Si_3N_4.

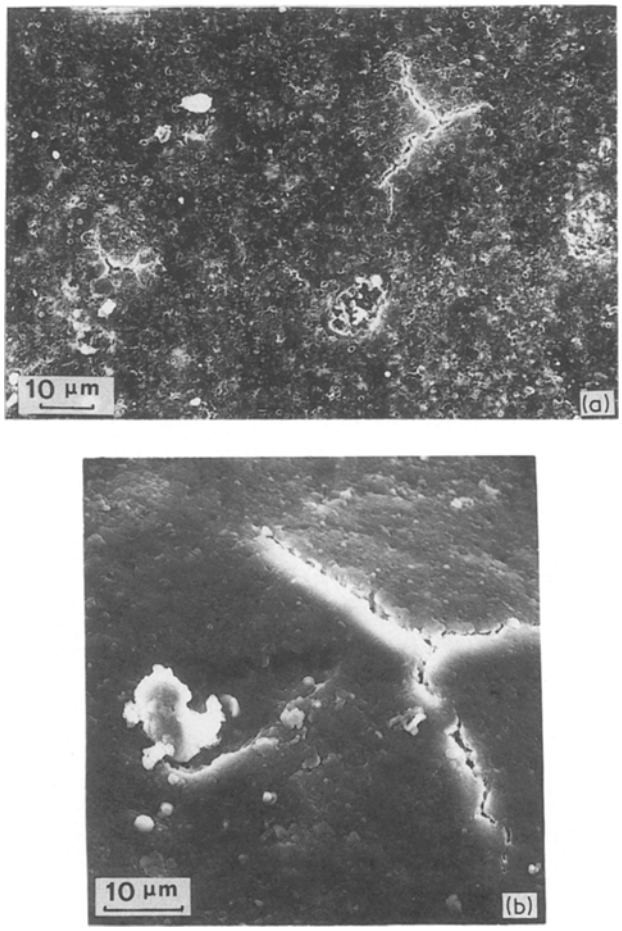

Figure 11 Morphological aspect of the surface of sample AZ after corrosion.

Silicon nitride does not react with liquid copper as copper nitride does not exist. The only possible reaction is the decomposition of silicon nitride according to the reaction

$$Si_3N_4 \rightarrow 3Si + 2N_2 \quad (1)$$

The equilibrium nitrogen partial pressure at 1400 K calculated from a ΔG^0 value equal to 67 351 cal (283 kJ) [19] and taking Si_3N_4 and silicon activities as one, is about 5×10^{-6} atm (0.5 Pa). As nitrogen is virtually insoluble in liquid copper, a nitrogen bubble must nucleate at the silicon nitride–copper interface. If the bubble nucleates at a pore or defect of about 1 μm diameter, an excess pressure inside the bubble exceeds 20 atm, according to the Laplace equation. Such pressure is much higher than the equilibrium pressure of reaction (1) so that it is reasonable to suppose that no decomposition of silicon nitride occurs in testing conditions.

These considerations can explain the very low corrosion noticed in A sample.

When zirconia is present (material AZ) there was no evidence of strong attack on the Si_3N_4 matrix and EPMA analyses showed a high enrichment of zirconium on the surfaces of the sample. Copper does not attack ZrO_2 so it can be inferred that a zirconia-reach passivating layer is established on the surface. The observed surface morphology may account for only a superficial phenomenon. The cracks could originate during cooling owing to a thermal mismatch among the phase constituting the surface layer and/or between these and the bulk. Moreover at about 1100° C the transformation of zirconia from tetragonal to monoclinic form occurs, with a volume increase ranging from 3 to 5%; giving rise to cracks and spallings.

The experimental evidence shows that materials A and AZ have an excellent resistance to molten copper.

It should be pointed out that even if M and MY types showed a more pronounced corrosion, its extent remained very small. We may conclude that hot pressed silicon nitride-based materials can be considered for use as a structural ceramic for molten copper metallurgical applications; however major improvements should have to be accomplished for the optimization of the starting composition for the specific application.

6. Concluding remarks

The corrosion resistance of various types of hot pressed silicon nitrides to molten copper has been evaluated.

The behaviour has been found to be related to the characteristics (chemical composition, type and amount) of secondary phases, whereas the silicon nitride phase seem mostly unaffected by liquid copper.

In all ceramics tested the extent of corrosion is very slight. However the materials hot pressed with Al_2O_3 as the sintering aid showed the best resistance to molten copper mainly because of the presence of the β'-sialon phase and the consequent very poor intergranular phase amount.

References

1. E. H. ANDREWS, *J. Mater. Sci.* **1** (1966) 377.
2. C. A. CALOW and R. B. BARCLAY, *ibid.* **2** (1967) 404.
3. E. H. ANDREWS, W. BONFIELD, C. K. DAVIES and A. J. MARKHAM, *ibid.* **7** (1972) 1003.
4. R. L. MEHAN and D. W. McKEE, *ibid.* **11** (1976) 1009.
5. M. J. BENNET and M. R. HOULTON, *ibid.* **14** (1979) 184.
6. T. W. LINDOP, *Chem. Eng.* **12** (1970) 427.
7. G. W. SAMSONOV and I. M. VINITSKII, "Handbook of Refractory Compounds" (IFI/Plenum, New York, 1980) p. 411.
8. K. H. JACK, *J. Mater. Sci.* **11** (1976) 1135.
9. L. A. LAY, "Corrosion Resistance of Technical Ceramics" (National Physical Laboratory, Teddington, 1983).
10. R. SANGIORGI, M. L. MUOLO and A. BELLOSI, *Mater. Sci. Eng.* **A103** (1988) 277.
11. C. N. BABINI, A. BELLOSI and P. VINCENZINI, *Ceramurgia* **14** (1984) 51.
12. A. BELLOSI, P. VINCENZINI and G. N. BABINI, *Mater. Chem. Phys.* **18** (1987) 205.
13. A. BELLOSI, P. VINCENZINI and G. N. BABINI, *J. Mater. Sci.* **23** (1988) 2348.
14. G. N. BABINI, A. BELLOSI and P. VINCENZINI, *ibid.* **17** (1982) 231.
15. G. N. BABINI, A. BELLOSI and C. GALASSI, *ibid.* **22** (1987) 1687.
16. R. SANGIORGI, M. L. MUOLO and R. MINISINI, *High Temp. Mater. Proc.* 1988, in press.
17. T. B. MASSALSKI (ed), "Binary Alloy Phase Diagrams", (A.S.M., Ohio, 1986).
18. G. N. BABINI, A. BELLOSI, R. CHIARA and M. BRUNO, *Adv. Ceram. Mater.* **2** (1987) 146.
19. I. BARIN and O. KNACKE, "Thermochemical Properties of Inorganic Substances" (Springer, Berlin, 1973).

Received 20 June
and accepted 7 December 1988